PHYSICAL REVIEW B VOLUME 48, NUMBER 20 15 NOVEMBER 1993-II

Current-voltage relation of a normal-metal–superconductor junction

Richard A. Riedel and Philip F. Bagwell
Purdue University, School of Electrical Engineering, West Lafayette, Indiana 47907
(Received 10 May 1993)

We calculate the electrical and heat currents flowing through a narrow, mesoscopic, normal-metal–superconductor (NS) junction containing a single point impurity. The NS junction exhibits large subgap conduction steps in its current-voltage (I-V) relation when the impurity is located in the normal metal. One new subgap step appears in the I-V characteristic whenever an additional quasiparticle is trapped between the impurity and NS interface. Locating the impurity inside the superconductor produces both an "excess current" and oscillations in the I-V characteristic analogous to the Tomasch effect. A maximum excess current of $2e\Delta/h$, slightly less than the $8e\Delta/3h$ found for a ballistic NS junction, is obtained when the impurity is located a few coherence lengths inside the superconductor.

INTRODUCTION

The Bogoliubov–de Gennes (BdG) equations[1–3] describe the coupled motion of electrons and time-reversed electrons. Coherent scattering of this quasiparticle, from both the superconducting "pairing potential" $\Delta(x)$ and the ordinary electrostatic potential $V(x)$, produces wave interference patterns in its motion. Introducing such an "impurity" potential $V(x)$ into a ballistic normal-metal–superconductor[3–8] or ballistic superconductor–normal-metal–superconductor[9–14] (SNS) junction therefore modifies the wave interference pattern of the quasiparticles in these junctions, changing the current-voltage (I-V) and/or current-phase (I-ϕ) characteristics of the junction. For example, an impurity in the SNS junction forces quasiparticles in the normal region to form standing waves near $\phi = \pi$, opening gaps in the energy-phase relationship[13] and suppressing the critical current of the Josephson junction.

An impurity also modifies the current-voltage relation of an NS junction.[3–8] Blonder, Tinkham, and Klapwijk (BTK) demonstrated[3] that a tunnel barrier, located at the NS interface, produces an I-V characteristic which interpolates smoothly between the tunnel junction ("dirty") and ballistic junction ("clean") limits. [The same electrostatic potential $V(x)$ can represent disorder, an insulating barrier (I), or a tunnel barrier.] We adopt the model and formalism of Ref. 3, but extend the calculation by allowing the impurity to exist anywhere inside the normal metal or superconductor. We assume that the superconducting order parameter is not degraded by either the impurity or the normal metal, and thus neglect the proximity effect. We also neglect the charge imbalance generated by quasiparticles entering the superconductor.

When the impurity is located inside the normal metal, forming a normal-metal–impurity normal-metal–superconductor (NINS) junction, the multiple Andreev reflections from the NS interface and normal reflections from the impurity produce long-lived quasibound states[15] inside the normal metal. These bound states give rise to sharp transmission resonances for energies inside the superconducting gap and to corresponding steps in the current-voltage relation for $eV \leq \Delta$. The subgap current carried by the quasibound states is large, of the same order of magnitude as the normal tunneling current. These quasibound quasiparticle states can also be observed in scanning tunneling microscope (STM) experiments.[16]

When the impurity is located inside the superconductor, producing a normal-metal–superconductor impurity superconductor (NSIS) geometry, a substantial "excess current"[3] appears in the I-V characteristic for $eV \gg \Delta$. Quasiparticles having energies outside the superconducting gap can no longer contribute significantly to the excess current $I_{\rm exc}$ in an NSIS geometry, so that $I_{\rm exc}$ is smaller in an NSIS junction than for a ballistic NS junction. In addition to this excess current, the multiple reflections of waves between the NS interface and the impurity also produce quasibound states inside the superconductor. The quasibound states in an NSIS junction only form outside the superconducting gap and are very short-lived because the Andreev reflection probability outside the gap is small. These weak transmission resonances produce correspondingly weak oscillations in the I-V curve for $eV \geq \Delta$, analogous to the Tomasch effect.[17]

Finally, we develop a transmission formalism to describe the heat current in NS junctions. Andreev reflection reduces the electronic entropy flowing into a superconductor, suppressing the heat current carried by the quasiparticles. For energies inside the superconducting gap, where the Andreev reflection is perfect, we show that no heat flows into the superconductor.

I. CURRENT-VOLTAGE CHARACTERISTICS

We solve for the motion of the quasiparticles using the BdG equation[1]

$$\begin{pmatrix} H(x)-\mu & \Delta(x) \\ \Delta^*(x) & -[H^*(x)-\mu] \end{pmatrix} \begin{pmatrix} u(x) \\ v(x) \end{pmatrix} = E \begin{pmatrix} u(x) \\ v(x) \end{pmatrix}, \tag{1}$$

where the one-electron Hamiltonian $H(x)$ is

$$H(x) = \frac{1}{2m}\left(-i\hbar\frac{d}{dx} - eA(x)\right)^2 + V(x), \tag{2}$$

and μ is the Fermi energy. We take the pairing potential $\Delta(x)$ to be a step function

$$\Delta(x) = \begin{cases} 0\,, & x<0 \\ \Delta e^{i\phi}\,, & x>0 \end{cases} \tag{3}$$

so that we ignore the proximity effect. We disorder the SN junction by placing a point impurity anywhere along the x-axis, namely

$$V(x) = V_i\delta(x-a). \tag{4}$$

The geometry corresponding to the potentials $\Delta(x)$ and $V(x)$ is shown in Fig. 1.

To calculate the current voltage relationship of the SN junction, we use the formalism of BTK.[3] We obtain the Andreev reflection probability $R_h(E)$ and normal reflection probability $R_e(E)$ using a scattering matrix technique[18] described in Appendix A. The energy dependence of $R_e(E)$ and $R_h(E)$ is discussed in Appendix B. The I-V characteristic is then found from[3]

$$I = \frac{2e}{h}\int_{-\infty}^{\infty}[f_N(E-eV)-f_S(E)] \times [1-R_e(E)+R_h(E)]\,dE\,. \tag{5}$$

We review the derivation of Eq. (5) in Appendix C.

Figure 2 shows the differential conductance dI/dV from Eq. (5) when the impurity is located in the normal metal. Large subgap transmission resonances having height $4e^2/h$, twice the value of the quantized ballistic conductance, are observed in dI/dV. Appendix B shows that there are approximately $(2L/\xi_0)$ of these subgap resonances, where $L \equiv |a|$ is the extent of the normal region and $\xi_0 = \hbar v_F/2\Delta$ is the Cooper pair size. An additional resonance therefore appears whenever the size of the normal region increases by a pair distance. The resonance width δV in voltage is approximately $e\delta V \simeq v_F T\hbar/4L$, where $T = 1 - R$ is the normal state transmission probability through the insulator.

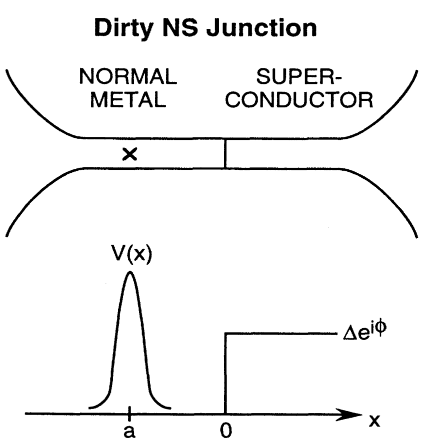

FIG. 1. Impurity potential $V(x)$ and pair potential $\Delta(x)$ used in this calculation. The point defect $V(x)$ can be located either in the superconductor or normal conductor.

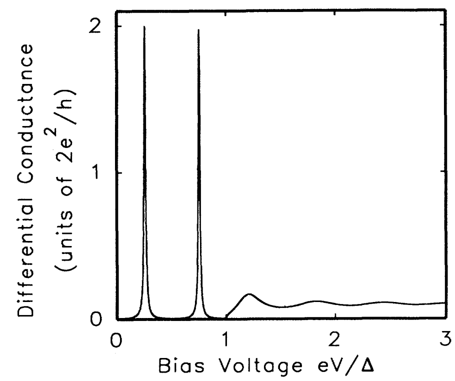

FIG. 2. Differential conductance for a NINS geometry, formed when the impurity resides in the normal metal (L = 100 nm). Each subgap ($eV < \Delta$) transmission resonance corresponds to an additional quasiparticle trapped between the impurity and superconductor.

The same dI/dV characteristic shown in Fig. 2 should be observable in STM experiments, for tunneling through a normal metal droplet on a superconductor.[16] The droplet must have a radius larger than the Cooper pair size ξ_0 to form the quasibound states. Only weak resonances in the dI/dV characteristic have been observed in STM experiments to date, presumably because electrons are tunneling into a two-dimensional film rather than a zero-dimensional droplet, and also due to the roughness of the normal metal film.

If the NINS structure is formed in a two-dimensional semiconductor layer, as is possible on InAs, no such resonant transmission (as shown in Fig. 2) should appear in the conductance (I/V) versus Fermi energy μ. For a normal conductor, dI/dV versus V and I/V versus μ show similar behavior. However, the resonant states formed inside the superconducting gap move with the Fermi energy and are not probed by conduction when $V \simeq 0$. The resonant states can be probed by a finite temperature.

Figure 3 shows the I-V characteristic, computed from Eq. (5), when the impurity is (a) in the normal metal and (b) inside the superconductor. The usual I-V characteristic for a tunnel junction[3] is obtained when the impurity is at the NS interface ($L = 0$) in Fig. 3(a). As we move the impurity away from the NS interface, sharp current steps appear in Fig. 3(a). These current steps again arise from quasibound states trapped between the impurity and the superconductor.

Subgap conduction due to the quasibound levels in Fig. 3(a) is substantial, having the same order of magnitude as the normal state tunneling current. This can

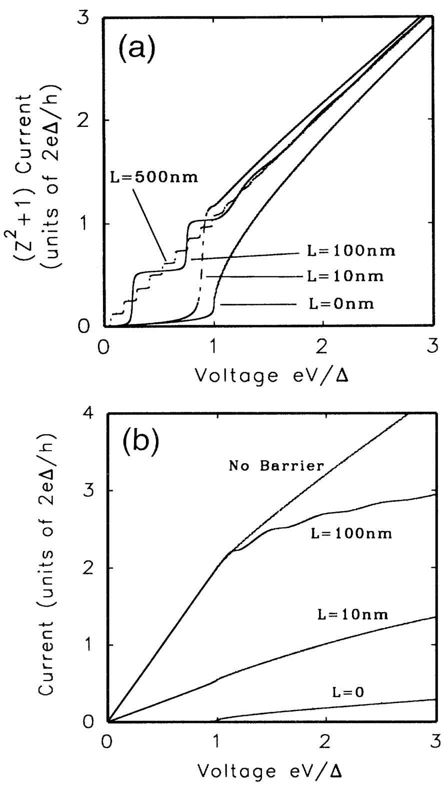

FIG. 3. Current-voltage characteristics of the SN junction when the impurity is (a) in the normal metal and (b) inside the superconductor. A large subgap current, due to conduction through resonant quasiparticle states, flows when the impurity is located in the normal metal. When the impurity is several coherence lengths inside the superconductor, the current reaches its ballistic value for $eV < \Delta$, but is limited by reflections from the impurity when $eV > \Delta$.

be reasoned as follows: The current carried by a single quasibound state is $(2e/h)\int(1-R_e+R_h)dE$, integrated over the resonance. The integral is approximately equal to the resonance width δE. Multiplying the number of resonances inside the gap times the current carried by each resonance gives the current flowing when the voltage is $eV = \Delta$ as

$$I \simeq (2e/h)(v_F T\hbar/4L)(2L/\xi_0) = (2e/h)T\Delta \ , \qquad (6)$$

approximately the same current as through a normal tunnel junction normal-metal–insulator normal metal (NIN). The electrical current through a normal-metal–insulator superconductor (NIS) tunnel junction near $eV = \Delta$ can thus be viewed as flowing through a single quasibound level near the gap edge.

Figure 3(b) shows the I-V relationship when the impurity is located in the superconductor. The main feature of Fig. 3(b) is the large increase in current as we move the scatterer further into the superconductor. When the impurity is at the NS interface, we obtain the usual "tunnel junction" I-V characteristic (lowest current). The largest current in Fig. 3(b) is for a ballistic NS junction, where the impurity strength $Z = V_i/\hbar v_F = 0$. When the impurity is well inside the superconductor ($L \gg \xi_0$), we recover the I-V characteristic for a clean NS junction for voltages $eV < \Delta$. This is due to conversion of the incident quasiparticle current to a supercurrent[3] for $E < \Delta$. However, for $E > \Delta$, this current conversion process is no longer effective, so that the current becomes limited by the impurity.

Due to this lack of current conversion outside the energy gap, the I-V curve for an NSIS junction at large voltages ($eV \gg \Delta$) has approximately the slope as the NIS or NIN tunnel junction I-V curve. In a clean NS junction, the excess current is composed of a contribution $2e\Delta/h$ from states inside the energy gap and an amount $2e\Delta/3h$ from states outside the energy gap. Placing a strong impurity in the superconductor eliminates the contribution from states outside the energy gap, reducing the excess current from $8e\Delta/3h$ to approximately $2e\Delta/h$ for an NSIS junction. (This conclusion holds only when the impurity is well inside the superconductor, i.e., $L \gg \xi_0$.)

When the impurity in an NSIS junction is less than a Cooper pair distance inside the superconductor ($L \leq \xi_0$), not all of the quasiparticle current is converted to supercurrent before reaching the impurity. The resulting I-V characteristic is intermediate between the tunnel junction (NIS) and NSIS junction having $L \geq \xi_0$. Figure 3(b) shows that the excess current is now smaller than $2e\Delta/h$ and the I-V characteristic no longer clearly displays the energy gap ($L = 10$ nm).

In our calculation, the I-V characteristic of the NSIS junction will always approach the result for a ballistic NS junction at low voltages when the impurity is well inside the superconductor, i.e., $eV < \Delta$ and $L \gg \xi_0$, regardless of the impurity strength. This counterintuitive result arises because we neglect the self-consistency condition for the order parameter. If the impurity is located in a narrow superconducting channel, it may be possible to depress the superconducting order parameter locally near the defect. In that case, some of the supercurrent will be converted back into normal current, and reflection from the impurity will again become effective. Thus, the BdG equations can be made to describe the standard "proximity effect" type of superconducting weak link. However, if the impurity is located inside the wide superconducting banks shown in Fig. 1, or if the order parameter is otherwise difficult to suppress, our calculation remains valid.[19]

II. HEAT CURRENT IN AN NS JUNCTION

The Andreev reflection process limits the electronic entropy which can flow into a superconductor.[21] Consider an electron incident on a superconductor inside its energy gap, carrying with it a given entropy current. To compensate for this entropy current attempting to flow into the superconductor, the superconductor ejects an equal amount of entropy current flowing in the opposite direction in the form of a hole. No net particle current, and therefore no net entropy current, can enter the superconductor. Unless an electron tries to transmit into the superconductor outside its energy gap, where it can enter the superconductor as a quasielectron, the superconductor does not permit its electronic entropy to increase. It is necessary that Andreev reflections limit the entropy flow into a superconductor, since a supercurrent itself carries no entropy, and since Andreev reflections inside the superconducting energy gap are the same as the motion of a Cooper pair.

The amount of entropy current and heat current carried by the quasiparticles can be computed in exactly the same way as for normal electrons in mesoscopic conductor.[22] The needed formalism, developed by Sivan and Imry,[22] can be understood[21] using the electron wave packet picture of Martin and Landauer.[23] Electron wave packets flowing out of a thermodynamic reservoir are interspersed with the absence of such packets at finite temperature. The entropy flow out of the reservoir is given by the logarithm of the number of different ways to arrange these packets. We modify the formalism of Ref. 22 to apply to an NS interface in Appendix D.

In the linear response limit, when the temperature difference and voltage difference between the two contacts are small compared to the average temperature, we find a heat current I_H of

$$I_H = \frac{2}{h}\int_{-\infty}^{\infty}(E-\tilde{\mu})[f_N(E-eV)-f_S(E)] \times [1-R_e(E)-R_h(E)]\,dE\,. \qquad (7)$$

The average electrochemical potential $\tilde{\mu}$ is determined by $\tilde{\mu} = (\mu_S+\mu_N)/2 = eV/2$. The factor $[1-R_e(E)-R_h(E)]$ in the integrand of Eq. (7) suppresses the heat current relative to a normal junction, just as the factor $[1-R_e(E)+R_h(E)]$ in the integrand of Eq. (5) enhances the electrical current relative to a normal junction. The factor $[1-R_e(E)-R_h(E)]$ in Eq. (7) is proportional to the particle current J_P, while the factor $[1-R_e(E)+R_h(E)]$ in Eq. (5) is proportional to the electrical current J_Q. We analyze the thermoelectric consequences of Eqs. (7) and (5) for the linear response limit in Appendix D.

Another interesting limit of transport is the nonlinear regime, where the bias voltage is large compared either to the average temperature or to the temperature difference between the contacts. An important quantity for heat flow in the nonlinear transport regime is the entropy S_B generated by scattering at a barrier, namely[21]

$$S_B = -k_B[T\ln T + R\ln R]\,. \qquad (8)$$

For the normal state transmission problem, the heat current flowing into either contact at large bias is approximately

$$I_H \simeq 2T_N S_B \frac{eV}{h}\,, \qquad (9)$$

where $T_N = T_S$ is the temperature of either contact. In this nonlinear regime of transport, only a small amount of entropy flows into the conductor at the Fermi energy from either contact, but a large amount of entropy and heat flow back into either contact due to entropy generation

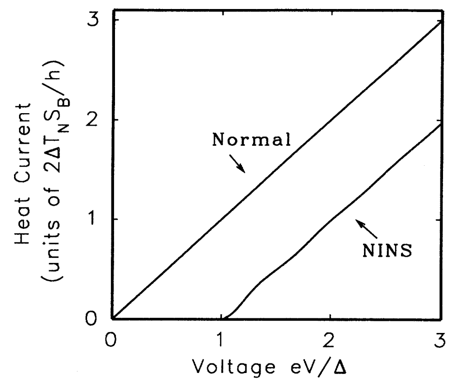

FIG. 4. Heat current flow in an NINS junction (having $L = 100$ nm) compared to the heat current flow in the normal state (NIN). Heat currents are completely suppressed by Andreev reflections inside the superconducting gap, producing a heat current deficit for $eV \gg \Delta$.

by the scattering obstacle. Equations (8) and (9) also follow from the analysis in Appendix D.

Figure 4 shows the heat current flowing into either contact in the nonlinear transport regime, normalized to that of Eq. (9). For normal contacts (NIN), the heat current closely follows Eq. (9). However, for the NINS junction a heat current deficit is evident at large voltages. This heat current deficit is simply Eq. (9) evaluated at $eV = \Delta$, so that heat currents flowing inside the superconducting energy gap are completely suppressed. The small oscillations in the heat current for the NINS case arise from wave interference of the quasiparticles in the normal region. The heat current flows in Fig. 4 and Appendix D are only the thermoelectric components, and have nothing to do with Joule heating.[24]

III. CONCLUSIONS

The tunneling Hamiltonian method explains the nonlinear I-V of an NIS junction by noting that, since there are no quasiparticle states available inside the superconducting energy gap, no current can tunnel into the superconductor. This type of reasoning breaks down for the ballistic NS junction, since the electrical current simply flows into the superconducting gap and is converted to a Cooper pair.[3] Our calculation provides a different perspective to explain the nonlinear I-V of an NIS tunnel junction. The tunnel junction carries little current at low voltages, $eV < |\Delta|$, because there are no resonant energy levels available to support the flow of quasiparticles. Since the insulating barrier is located directly at the NS interface in a tunnel junction, the lowest energy quasibound state occurs at $E = \Delta$. Therefore, the smallest voltage at which electrical current can flow is $eV = \Delta$. The superconducting tunnel junction conducts primarily through a resonant state at the gap edge near $eV \simeq \Delta$, so that the nonlinear I-V characteristic of an NIS tunnel junction (Giaever tunneling) must itself be considered a mesoscopic phenomenon.

If we move the tunnel barrier away from the NS interface, forming a NINS junction, a resonant Andreev level can exist between the impurity and superconductor for energies $E < |\Delta|$. The electrical current is carried through these resonances when $eV \leq \Delta$, producing a new subgap step in the I-V characteristic whenever an additional quasiparticle can fit resonantly between the tunnel barrier and the NS interface. The total electrical current carried by the quasibound states in an NIS or NINS junction is approximately equal to the normal state tunneling current at $eV = \Delta$, namely $I = e\Delta T/h$. These quasibound levels therefore carry a sizeable electrical current.

For energies outside the superconducting gap, no resonance condition need be enforced in order for electrical current to flow in an NIS or NINS junction. This is because the superconductor no longer strongly confines electronic states outside its gap. A scattering state inside the superconductor can then simply carry the quasiparticles away from the NS junction when $E > |\Delta|$, permitting good electrical conduction when $eV > |\Delta|$. The electrical current per unit energy carried by scattering states outside the energy gap is approximately the same as for a normal conductor. Combining the scattering state current and bound state current gives approximately the same total current in an NINS junction as for a normal (NIN) tunnel junction when $eV \geq \Delta$. We find, however, that the "gap edge" in the I-V curve near $eV = \Delta$ can be somewhat blurred if the impurity is not located exactly at the NS interface. One cannot accurately infer the superconducting gap by tunneling measurements in that case.

Our calculation gives further insight into the conversion of normal current to supercurrent in a dirty superconductor or NSIS junction. Incident quasiparticle currents are only converted to supercurrents (when the source term in the BdG conservation laws is the only mechanism available for such conversion) for energies inside the superconducting gap. Outside the gap, the incident quasiparticle currents remain as quasiparticle currents and are not converted to a supercurrent. This lack of current conversion outside the gap is observed in the I-V characteristic of an NSIS junction if the impurity is several Cooper pair distances inside the superconductor. In such an NSIS junction, the electrical current for $eV < \Delta$ approaches that of a ballistic NS junction, while the differential conductance dI/dV for $eV > \Delta$ approaches that of the normal tunnel junction (NIN). The excess current is then limited to approximately $2e\Delta/h$ for such a dirty superconductor or NSIS junction.

Although Andreev reflections enhance the electrical current at an NS interface, they suppress the electronic entropy flow and heat flow into the superconductor. A corresponding heat current deficit appears at large voltages in the NINS junction. The transmission formalism we used to calculate the thermoelectric properties of the NIS junction can be applied to many other thermoelectric transport properties of superconductors.

ACKNOWLEDGMENTS

We thank Erkan Tekman for useful discussions. We gratefully acknowledge support from the David and Lucile Packard Foundation and from the Indiana Center for Innovative Superconductor Technology.

APPENDIX A: PARTICLE CURRENT SCATTERING MATRIX

The particle current J_P and electrical current J_Q are determined from Eq. (1), as Eq. (1) embodies the two conservation laws[2,3]

$$\nabla \cdot \mathbf{J}_P + \frac{\partial P}{\partial t} = 0 \tag{A1}$$

and

$$\nabla \cdot \mathbf{J}_Q + \frac{\partial Q}{\partial t} = S\ . \tag{A2}$$

Here P is the density of both ordinary and time-reversed particles

$$P(x) = |u(x)|^2 + |v(x)|^2 \tag{A3}$$

and is coupled to the conserved particle current J_P, where

$$\mathbf{J}_P(x) = \frac{\hbar}{m}\mathrm{Im}\,\{u(x)^*[\nabla u(x)] - v(x)^*[\nabla v(x)]\}\ . \tag{A4}$$

Q is the density of particles relevant to electronic transport, namely the particle density minus the density of time-reversed particles

$$Q(x)/e = |u(x)|^2 - |v(x)|^2\ . \tag{A5}$$

The effective transport charge density Q is coupled to an electrical current J_Q, with

$$\mathbf{J}_Q(x) = \frac{e\hbar}{m}\mathrm{Im}\,\{u(x)^*[\nabla u(x)] + v(x)^*[\nabla v(x)]\}\ . \tag{A6}$$

The source term S has the form

$$S(x) = \frac{4e}{\hbar}\mathrm{Im}\,[u(x)^*\Delta(x)v(x)]\ . \tag{A7}$$

We use a scattering matrix technique[18] to obtain the particle current amplitude j_P everywhere, and hence the particle current $J_P = j_P^* j_P$. As in Fig. 1 of Ref. 18, let a denote the particle current amplitudes to the left of the scattering obstacle and b denote those to the right. We wish to calculate the scattering matrix S which connects the incoming particle current amplitudes a^+ and b^- to the outgoing particle current amplitudes b^+ and a^- according to

$$\begin{bmatrix} b^+ \\ a^- \end{bmatrix} = \begin{bmatrix} t & r' \\ r & t' \end{bmatrix} \begin{bmatrix} a^+ \\ b^- \end{bmatrix}. \tag{A8}$$

The b^+, a^-, a^+, and b^- are two component column vectors. The upper component is the amplitude for electronlike particles and the lower component is the amplitude of the holelike (time-reversed) particles. The matrix elements t, t', r, and r' are each themselves 2×2 matrices. Diagonal elements of the submatrices t, t', r, and r' correspond to normal reflection and transmission, while off-diagonal elements correspond to Andreev reflections or transmission with branch crossing.

The individual scattering matrices for the different regions are found using the BdG equations. Let k be the wave vector inside the normal metal

$$k_\pm = \sqrt{\frac{2m}{\hbar^2}(\mu \pm E)} \tag{A9}$$

and q the wave vector inside the superconductor

$$q_\pm = \sqrt{\frac{2m}{\hbar^2}\left(\mu \pm \sqrt{E^2 - |\Delta|^2}\right)} \,. \tag{A10}$$

To match the wave function and its derivative everywhere, we use Andreev's approximation that all wave vectors are approximately equal. This approximation is valid when $\mu \gg \Delta$. We therefore take $q^+ \simeq q^- \simeq k^+ \simeq k^-$ except in an exponent.

For the impurity potential $V(x)$ we find the scattering matrices

$$t = t' = \begin{bmatrix} \frac{1}{1+iZ} & 0 \\ 0 & \frac{1}{1-iZ} \end{bmatrix}, \qquad r = r' = \begin{bmatrix} \frac{-iZ}{1+iZ} & 0 \\ 0 & \frac{iZ}{1-iZ} \end{bmatrix}, \tag{A11}$$

where Z is the dimensionless barrier strength $Z = V_i/\hbar v_F$. The normal state transmission coefficient T related to Z by $T = 1 - R = 1/(1+Z^2)$. Equation (A11) holds when the impurity is located in either the normal metal or superconductor.

For a region of free propagation in the normal metal we have

$$t = \begin{bmatrix} e^{ik_+L} & 0 \\ 0 & e^{-ik_-L} \end{bmatrix} = t', \qquad r = r' = \begin{bmatrix} 0 & 0 \\ 0 & 0 \end{bmatrix}, \tag{A12}$$

where $L > 0$ is the size of the region. To describe a region of free propagation in the superconductor we replace $k_+ \to q_+$ and $k_- \to q_-$ in Eq. (A12).

The scattering matrix for the NS interface is

$$t = \sqrt{|u_0|^2 - |v_0|^2}\begin{bmatrix} \frac{e^{-i\phi}}{u_0} & 0 \\ 0 & \frac{1}{u_0} \end{bmatrix}, \qquad t' = \frac{u_0^2 - v_0^2}{\sqrt{|u_0|^2 - |v_0|^2}}\begin{bmatrix} \frac{e^{i\phi}}{u_0} & 0 \\ 0 & \frac{1}{u_0} \end{bmatrix} \tag{A13}$$

and

$$r = \begin{bmatrix} 0 & \frac{v_0}{u_0}e^{i\phi} \\ \frac{v_0}{u_0}e^{-i\phi} & 0 \end{bmatrix}, \qquad r' = \begin{bmatrix} 0 & -\frac{v_0}{u_0} \\ -\frac{v_0}{u_0} & 0 \end{bmatrix}. \tag{A14}$$

Here ϕ is the phase of the superconducting order parameter. The u_0 and v_0 are standard "coherence" factors

$$u_0 = \sqrt{\frac{1}{2}\left(1 + \frac{\sqrt{E^2 - |\Delta|^2}}{E}\right)} \tag{A15}$$

and

$$v_0 = \sqrt{\frac{1}{2}\left(1 - \frac{\sqrt{E^2 - |\Delta|^2}}{E}\right)} \,. \tag{A16}$$

The scattering matrix for the electrical current amplitude j_Q, where the electrical current is $J_Q = j_Q^* j_Q$, can be obtained by sending $\sqrt{|u_0|^2 - |v_0|^2} \to \sqrt{|u_0|^2 + |v_0|^2}$ in Eq. (A13).

The overall scattering matrix S is obtained by combining the scattering matrices of each successive region

$$S = S_1 \otimes S_2 \otimes S_3 \,. \tag{A17}$$

The symbol $\otimes$ denotes combining the scattering matrices according to their compostion law.[18] If $S = S_1 \otimes S_2$, then

$$t = t_2 \left[I - r_1' r_2\right]^{-1} t_1 \,, \tag{A18}$$

$$r = r_1 + t_1' r_2 \left[I - r_1' r_2\right]^{-1} t_1 \,, \tag{A19}$$

$$t' = t_1' \left[I + r_2 \left[I - r_1' r_2\right]^{-1} r_1'\right] t_2' \,, \tag{A20}$$

$$r' = r_2' + t_2 \left[I - r_1' r_2\right]^{-1} r_1' t_2' \,. \tag{A21}$$

Let the transmission probability for the quasiparticle current J_P of an electron incident from the normal conductor onto the superconductor be T_e for normal transmission, R_e for normal reflection, R_h for Andreev reflection, and T_h for transmission with branch crossing. Then let T_e', R_e', R_h', and T_h' denote same quantities for a quasielectron incident from the superconductor. Equations (A17)–(A21) then determine the needed particle current transmission and reflection coefficients from $R_e = r_e r_e^*$, $R_h = r_h r_h^*$, $T_e = t_e t_e^*$, and $T_h = t_h t_h^*$. We find that the detailed balancing condition $T_e = T_e'$ and

$T_h = T'_h$ holds.[3] Further, the S matrices are unitary so that $1 = R_e + R_h + T_e + T_h$ and $1 = R'_e + R'_h + T'_e + T'_h$.

When the impurity is in the normal metal, we find from Eqs. (A17)–(A21)

$$r_e = \frac{1}{d}\left(\frac{-iZ}{1+iZ}\right)\left[1-\left(\frac{v_0}{u_0}\right)^2 e^{2i(k_+-k_-)L}\right] , \quad \text{(A22)}$$

$$r_h = \frac{1}{d}\left(\frac{v_0}{u_0}\right)\left(\frac{1}{1+Z^2}\right) e^{-i\phi}e^{i(k_+-k_-)L} , \quad \text{(A23)}$$

$$t_e = \left(\frac{\sqrt{|u_0|^2-|v_0|^2}}{d}\right)\left(\frac{e^{-i\phi}e^{ik_+L}}{u_0(1+iZ)}\right) , \quad \text{(A24)}$$

$$t_h = \left(\frac{\sqrt{|u_0|^2-|v_0|^2}}{d}\right)\left(\frac{v_0}{u_0}\right)\left(\frac{e^{-i\phi}e^{ik_+L}}{u_0(1+iZ)}\right) \times\left(\frac{iZ}{1-iZ}\right)e^{-2ik_-L} , \quad \text{(A25)}$$

and

$$d = 1-\left(\frac{Z^2}{1+Z^2}\right)\left(\frac{v_0}{u_0}\right)^2 e^{2i(k_+-k_-)L} . \quad \text{(A26)}$$

Results similar to Eqs. (A22)–(A26) were obtained in Refs. 4 and 5.

A calculation analogous to Eqs. (A22)–(A26) can be performed when the impurity resides inside the superconductor. Equations (A17)–(A21) then give

$$r_e = \left(\frac{-iZ}{1+iZ}\right)\left[1-\left(\frac{v_0}{u_0}\right)^2\right]\frac{e^{2iq_+L}}{d} , \quad \text{(A27)}$$

$$r_h = \left[1-\left(\frac{Z^2}{1+Z^2}\right)e^{2i(q_+-q_-)L}\right]\left(\frac{v_0}{u_0}e^{-i\phi}\right)\left(\frac{1}{d}\right) , \quad \text{(A28)}$$

$$t_e = \frac{\sqrt{|u_0|^2-|v_0|^2}}{d}\left(\frac{e^{-i\phi}e^{iq_+L}}{u_0(1+iZ)}\right) , \quad \text{(A29)}$$

$$t_h = \frac{\sqrt{|u_0|^2-|v_0|^2}}{d}\left(-\frac{v_0}{u_0}\right)\left(\frac{e^{-i\phi}e^{-iq_-L}}{u_0(1-iZ)}\right) \times\left(\frac{-iZ}{1+iZ}\right)e^{2iq_+L} , \quad \text{(A30)}$$

and

$$d = 1-\left(\frac{Z^2}{1+Z^2}\right)\left(\frac{v_0}{u_0}\right)^2 e^{2i(q_+-q_-)L} . \quad \text{(A31)}$$

A quasibound state is defined as a complex energy pole of the current transmission amplitude.[15] Setting $d = 0$ in Eqs. (A26) and (A31) determines these poles and therefore determines the bound and quasibound states of the scattering potential. When the impurity is in the normal metal, Eq. (A26) requires

$$\left(\frac{Z^2}{1+Z^2}\right)\left(\frac{v_0}{u_0}\right)^2 e^{2i(k_+-k_-)L} = 1 , \quad \text{(A32)}$$

while Eq. (A31) enforces

$$\left(\frac{Z^2}{1+Z^2}\right)\left(\frac{v_0}{u_0}\right)^2 e^{2i(q_+-q_-)L} = 1 , \quad \text{(A33)}$$

when the impurity is in the superconductor. A complex energy $E = E_R + iE_I$ is required to solve Eq. (A32) and (A33), where E_R is the energy of the resonance and $\hbar/|E_I|$ its lifetime. The left-hand sides of Eqs. (A32) and (A33) can be interpreted as the product of probability amplitudes for an electron moving from the impurity to the NS interface, Andreev reflecting as a hole, the hole returning to the impurity, normally reflecting, propagating back the NS interface, Andreev reflecting as an electron, returning again to the impurity, and normally reflecting as an electron.

APPENDIX B: TRANSMISSION COEFFICIENTS

We graph the transmission and reflection coefficients for the particle currents J_P in Fig. 5. The electron energy is measured relative to the Fermi energy in the superconductor. In Fig. 5(a), the impurity is located in the normal metal. The Andreev reflection probability R_h shows resonant peaks inside the superconducting gap ($E < \Delta$), while the normal reflection probabilty R_e is suppressed near these resonances. The resonances are well described by Eq. (A32), which requires

$$2\pi i n \simeq \ln R + 2i\cos^{-1}([E_R + iE_I]/\Delta) + 2i([E_R + iE_I]/\Delta)(L/\xi_0) . \quad \text{(B1)}$$

For opaque barriers having $R \simeq 1$, we find the positions E_R of the bound levels are approximately determined by

$$2\cos^{-1}\left(\frac{E_R}{\Delta}\right) + \left(\frac{2L}{\xi_0}\right)\left(\frac{E_R}{\Delta}\right) \simeq 2\pi n , \quad \text{(B2)}$$

while the leakage rate $2E_I/\hbar$ is set approximately as

$$\frac{2E_IL}{\Delta\xi_0} \simeq \ln R \simeq -T . \quad \text{(B3)}$$

Note that $E_I < 0$, as required for the linear system to be stable.

Equation (B2) is similar to the condition for Andreev bound levels in an SNS junction,[13] except that the Andreev bound levels in the NS junction are leaky. The width of the transmission resonances is limited by the partial leakage through the impurity, so the resonance lifetime is approximately $\hbar/2|E_I| \simeq 2L/v_FT$. For larger values of L more resonances appear in the Andreev reflection, approximately one new resonance whenever L increases by ξ_0.

We can now explain Fig. 5(a) qualitatively. In a clean NS junction, only Andreev reflection occurs inside the superconducting energy gap. In the NINS junction, Andreev reflection occurs inside the energy gap only if the resonance condition (A32) is met. On resonance, the scattering potential can accommodate a new quasiparticle between the impurity and superconductor. An electron can then reach the superconductor and reflect as a hole. If the resonance condition (A32) is not met, no waves can propagate to the superconductor, and electrons mostly reflect as electrons inside the energy gap.

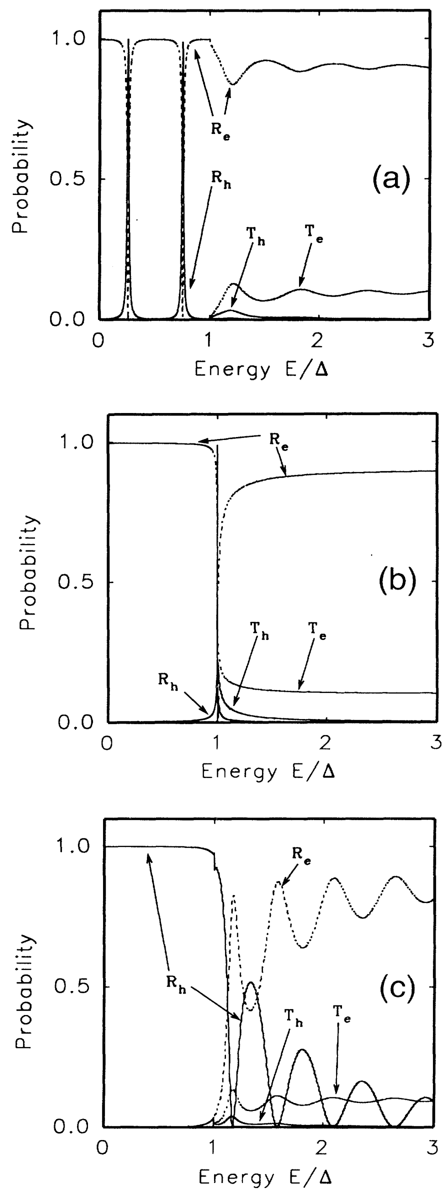

FIG. 5. Transmission coefficients versus energy, when the impurity is (a) in the normal metal ($L = 100$ nm), (b) at the SN interface ($L = 0$ nm), and (c) inside the superconductor ($L = 100$ nm). The oscillating transmission arises from quasibound states forming between the impurity and SN interface.

Outside the energy gap there is little Andreev reflection, so that no resonance condition is strongly enforced. Incident electrons then either transmit or reflect mostly as electrons, according to their corresponding probability for doing so in the normal state.

Some weaker resonances in R_h outside the superconducting energy gap are also visible in Fig. 5(a). For an energy E_R near the gap edge, and for a long junction having $L \gg \xi_0$, we find the approximate poles of the transmission amplitude at an energy $E = E_R + iE_I$, with

$$\frac{2E_R L}{\Delta\xi_0} \simeq 2\pi n \ , \tag{B4}$$

and a resonance width $|E_I|$ determined from

$$\frac{2E_I L}{\Delta\xi_0} \simeq \ln(RR_a) \ . \tag{B5}$$

Here $R_a = |v_0/u_0|^2$ is the Andreev reflection probability of the clean NS junction, evaluated at $E = E_R$. The large width of the transmission resonances outside the superconducting gap in Fig. 5(a) is not due to a very transmissive impurity, but is instead due to the relatively weak Andreev reflection probability R_a outside the superconducting gap. Even though the potential barrier may be effective at confining an electron, the pair potential discontinuity is no longer effective at confining the electron, increasing the resonance width to approximately $2|E_I| \simeq \hbar v_F(T + 1 - R_a)/2L$ near the gap edge. Since the Andreev reflection probability R_a continually decreases as the electron energy moves further outside the gap, the resonances eventually disappear at large energy. These weak resonances outside the superconducting gap carry the "continuum" contribution to the Josephson current in a long SNS junction.[13]

When the impurity is located exactly at the NS interface, as in Fig. 5(b), the transmission coefficients show a single Andreev resonance at the energy gap of the superconductor.[3] This single quasibound state has the same origin as the single bound state responsible for the discretization of the supercurrent in a quantum point contact,[20] i.e., Eq. (B2) with $L = 0$ is similar to the point contact bound states. At least one bound state is always possible because the wave functions have a finite decay length $\xi(E)$ inside the superconductor, producing an effective potential well of size $\xi(E) = \xi_0\Delta/\sqrt{E^2 - \Delta^2}$.

As we move the impurity inside the superconductor, corresponding to Fig. 5(c), Andreev reflections inside the superconducting gap begin to increase while the normal reflections decrease. In Fig. 5(c), for example, electron reflection R_e inside energy gap is negligible, while $R_h \simeq 1$. This change is due to the conversion of normal current to supercurrent within a length $\xi(E)$ of the NS interface.[3] By the time the impurity is several ξ_0 inside the superconductor, essentially all the quasiparticle (normal) current is converted to a supercurrent before it reaches the impurity. As in Fig. 5(c), normal reflections inside the gap are then completely suppressed. The impurity is therefore essentially absent for electrons incident inside the superconducting gap.

However, for electrons incident on the superconductor outside the gap, normal reflections from the impurity are effective, no matter how far the impurity is removed from the NS interface. This is because conversion from quasiparticle current to supercurrent is no longer effective outside the superconducting gap. The source term S in the BdG electrical current conservation law, Eq. (A7), is either zero or oscillates as a function of position. The integral $-\int S(x)dx \equiv J_S$, which converts quasiparticle electrical currents J_Q to supercurrents J_S, therefore gives no net current conversion outside the gap. Electrical currents carried outside the superconducting energy gap (for particles incident on the superconductor from the normal metal) are therefore purely quasiparticle currents and can be reflected by a scattering obstacle.

Oscillations in the transmission coefficients above the gap also begin to appear when the impurity is several ξ_0 inside the superconductor, as in Fig. 5(c). These oscillations again arise from quasibound states inside the superconductor, found from the complex energy poles of Eq. (A33). Using the equality $q_+ - q_- \simeq k_F(\sqrt{E^2 - |\Delta|^2}/\mu)$, the required condition is

$$\ln(RR_a) + 2i\frac{L}{\Delta\xi_0}\sqrt{(E_R + iE_I)^2 - |\Delta|^2} \simeq 2\pi i n \,. \quad \text{(B6)}$$

We find the resonances at an energy E_R

$$E_R^2 \simeq |\Delta|^2 + \left(\frac{\pi n}{L}\right)^2 (\Delta\xi_0)^2 \quad \text{(B7)}$$

and a resonance width $|E_I|$ determined from

$$E_I \simeq \frac{\pi n}{2E_R}\left(\frac{\Delta\xi_0}{L}\right)^2 \ln(RR_a) \,. \quad \text{(B8)}$$

These same resonances were previously observed in the Tomasch effect.[17]

APPENDIX C: ELECTRICAL CURRENT BALANCE

Equation (5) implies detailed balance for the electrical current in an SN junction, i.e., it requires electrical current balance at each individual energy. BTK (Ref. 3) used a transmission formalism to compute the electrical current due to quasiparticles incident from the normal side of the NS junction. BTK then effectively invoked time-reversal symmetry to obtain Eq. (5), i.e., they implicitly assumed detailed electrical current balance holds at each individual energy. However, the transmission formalism of van Wees, Lenssen, and Harmans[11] allows us to actually compute the electrical current carried by the quasiparticles incident from the superconducting side of the NS junction. After performing this calculation, we indeed find detailed balance for the particle current,[3] but not for the electrical current.

Consider the simplest case of a ballistic NS junction ($Z = 0$). We also limit the discussion to $E > \Delta$. (Interchange $|v_0|^2$ and $|u_0|^2$ to extend the discussion to $E < -\Delta$.) The particle current per unit energy flowing from the normal side is

$$J_P^{\rightarrow}(E)N_N^+(E) = \frac{2}{h}\left(1 - \frac{|v_0|^2}{|u_0|^2}\right) \quad \text{(C1)}$$

and the electrical current per unit energy is

$$J_Q^{\rightarrow}(E)N_N^+(E) = \frac{2e}{h}\left(1 + \frac{|v_0|^2}{|u_0|^2}\right) \,. \quad \text{(C2)}$$

The normal density of states for rightmoving electrons is $N_N^+(E) = 1/v_F h$. In contrast, the particle and electrical current per unit energy flowing from the superconducting side are

$$eJ_P^{\leftarrow}(E)N_S^-(E) = J_Q^{\leftarrow}(E)N_S^-(E) = \frac{2e}{h}\left(1 - \frac{|v_0|^2}{|u_0|^2}\right) \,. \quad \text{(C3)}$$

The density of states for leftmoving quasiparticles in the superconductor is $N_S^-(E) = 1/v_F h(|u_0|^2 - |v_0|^2)$.

Equations. (C1)–(C3) show the detailed balance of the quasiparticle current J_P and the detailed imbalance of the electrical current J_Q. Similar difficulties arise for the NINS and NSIS junctions. The incident wave functions in both the normal metal and superconductor have a normalization $P = 1$, i.e., one quasiparticle per available state. Changing the normalization of the states cannot bring both the quasiparticle and electrical current into detailed balance. One should be able to derive Eq. (5) of BTK (Ref. 3) from an electrical current transmission approach,[11] but we have been unable to do so. Equation (7) for the heat flow we have obtained from a transmission formalism.

APPENDIX D: THERMOELECTRIC HEAT CURRENTS

We modify the entropy current formalism of Sivan and Imry[22] to apply to the NS boundary. To do this, we regard the electronlike and holelike particles as two physically distinct "channels" and sum their contribution to the entropy flow. (One must divide the total entropy flow by a factor of 2 at the end of the calculation to compensate for overcounting the total number of states in the conductor.) Both electrons and holes incident from the normal side are taken to be in equilibrium with the Fermi occupation factor f_N for the normal metal reservoir, while those injected from the superconductor are distributed in energy according to the Fermi factor f_S.

The total entropy flowing out of the normal reservoir is therefore

$$S_N^{\text{out}} = -k_B\left[f_N \ln f_N + (1 - f_N)\ln(1 - f_N)\right] \,. \quad \text{(D1)}$$

The entropy associated with quasiparticles flowing back into the normal contact is

$$S_N^{\rm in}/(-k_B) = [(R_e+R_h)f_N + (T_e'+T_h')f_S]\ln[(R_e+R_h)f_N + (T_e'+T_h')f_S] + [1-(R_e+R_h)f_N - (T_e'+T_h')f_S] \times \ln[1-(R_e+R_h)f_N - (T_e'+T_h')f_S] \ . \tag{D2}$$

The net heat current $I_{H,N}$ flowing out of the normal reservoir is then, including spin,

$$I_{H,N} = 2T_N \int [S_N^{\rm out} - S_N^{\rm in}]\frac{dE}{h} \ . \tag{D3}$$

T_N is the temperature of the normal contact.

Computation of the entropy and heat current flowing into the superconductor proceeds in the same fashion. The entropy carried by quasiparticles flowing out of the superconductor is

$$S_S^{\rm out} = -k_B\,[f_S\ln f_S + (1-f_S)\ln(1-f_S)] \ . \tag{D4}$$

Quasiparticles flowing back into the superconductor carry an entropy

$$S_S^{\rm in}/(-k_B) = [(R_e'+R_h')f_S + (T_e+T_h)f_N]\ln[(R_e'+R_h')f_S + (T_e+T_h)f_N] + [1-(R_e'+R_h')f_S - (T_e+T_h)f_N] \times \ln[1-(R_e'+R_h')f_S - (T_e+T_h)f_N] \ . \tag{D5}$$

The total heat current $I_{H,S}$ flowing into the superconducting reservoir is then

$$-I_{H,S} = 2T_S \int [S_S^{\rm out} - S_S^{\rm in}]\frac{dE}{h} \ . \tag{D6}$$

Equations (D1)–(D6) can be evaluated in the linear response regime. Take the average temperature $\tilde{T}$ as $\tilde{T} = (T_S+T_N)/2$ and the average electrochemical potential $\tilde{\mu}$ as $\tilde{\mu} = (\mu_S+\mu_N)/2 = eV/2$. The temperature difference is $\triangle T = T_N - T_S$ and electrochemical potential difference is $\triangle\mu = \mu_N - \mu_S = eV$. The Fermi factors can be written as $f_N = f + \triangle f$ and $f_S = f - \triangle f$, where f is the average Fermi distribution set by $\tilde{\mu}$ and $\tilde{T}$. The essential approximation for the linear response regime is that $\triangle f \ll f$, which holds if $\tilde{T} \gg \triangle T$, $k_B\tilde{T} \gg eV$, and $\tilde{\mu} \gg \tilde{T}$. Linearizing either Eq. (D3) or Eq. (D6) in $\triangle f$, we find $I_{H,N} = -I_{H,S} = I_H$ given by Eq. (7). The electrical current is still found from Eq. (5).

For small voltage differences V and small temperature differences $\triangle T$, Eqs. (5) and (7) can be cast into the form

$$I \simeq GV + L(\triangle T) \tag{D7}$$

and

$$I_H \simeq G_H V + L_H(\triangle T) \ . \tag{D8}$$

The linear response coefficients G, L, G_H, and L_H are

$$G = \frac{2e^2}{h}\int (1-R_e+R_h)\left(-\left.\frac{df}{dE}\right|_{\tilde{\mu},\tilde{T}}\right)dE \ , \tag{D9}$$

$$L = \frac{1}{\tilde{T}}\frac{2e}{h}\int (1-R_e+R_h)(E-\tilde{\mu})\left(-\left.\frac{df}{dE}\right|_{\tilde{\mu},\tilde{T}}\right)dE \ , \tag{D10}$$

$$G_H = \frac{2e}{h}\int (1-R_e-R_h)(E-\tilde{\mu})\left(-\left.\frac{df}{dE}\right|_{\tilde{\mu},\tilde{T}}\right)dE \ , \tag{D11}$$

and

$$L_H = \frac{1}{\tilde{T}}\frac{2}{h}\int (1-R_e-R_h)(E-\tilde{\mu})^2\left(-\left.\frac{df}{dE}\right|_{\tilde{\mu},\tilde{T}}\right)dE \ , \tag{D12}$$

analogous to Ref. 22. G and L are enhanced relative to the normal state, while G_H and L_H are strongly suppressed. The thermal conductivity L_H in Eq. (D12) can be evaluated for any type of scattering potential, including the problem of thermal conduction in the type-I intermediate state of a superconductor originally studied by Andreev.[25] A transmission calculation of the heat flow, analogous to the one in this appendix, can also be performed for a Josephson junction.[26]

[1] P.G. de Gennes, *Superconductivity of Metals and Alloys* (Addison-Wesley, New York, 1989).
[2] W.N. Mathews, Jr., Phys. Status Solidi B **90**, 327 (1978).
[3] G.E. Blonder, M. Tinkham, and T.M. Klapwijk, Phys. Rev. B **25**, 4515 (1982).
[4] A. Hahn, Phys. Rev. B **31**, 2816 (1985).
[5] P.C. van Son, H. van Kempen, and P. Wyder, Phys. Rev. B **37**, 5015 (1988).
[6] B.J. van Wees, P. de Vries, P. Magnee, and T.M. Klapwijk, Phys. Rev. Lett. **69**, 510 (1992).

[7] Y. Takane and H. Ebisawa, J. Phys. Soc. Jpn. **61**, 1685 (1992).
[8] C.W.J. Beenakker, Phys. Rev. B **46**, 12 841 (1992).
[9] J. Bardeen and J.L. Johnson, Phys. Rev. B **5**, 72 (1972).
[10] C.W.J. Beenakker, Phys. Rev. Lett. **67**, 3836 (1991).
[11] B.J. van Wees, K.M.H. Lenssen, and C.J.P.M. Harmans, Phys. Rev. B **44**, 470 (1991).
[12] A. Furusaki, H. Takayanagi, and M. Tsukada, Phys. Rev. B **45**, 10 563 (1992).
[13] P.F. Bagwell, Phys. Rev. B **46**, 12 573 (1992).
[14] G. Rittenhouse and J. Graybeal, Phys. Rev. B (to be published).
[15] P.F. Bagwell and R.K. Lake, Phys. Rev. B **46**, 15 329 (1992).
[16] S.H. Tessmer, D.J. van Harlingen, and J.W. Lyding, Phys. Rev. Lett. **70**, 3135 (1993).
[17] T. Wolfram, Phys. Rev. **170**, 481 (1968).
[18] M. Cahay, M. McLennan, and S. Datta, Phys. Rev. B **37**, 10 125 (1988).
[19] The parameters used in the calculation are $\mu = 1$ eV, $|\Delta| = 10$ meV, $Z = 3$, and m is the free electron mass. These parameters determine the normal state transmission coefficient $T = 0.1$, the Fermi wavelength $\lambda_F = 12.3$ Å, and the coherence length $\xi_0 = 196$ Å.
[20] C.W.J. Beenakker and H. van Houten, Phys. Rev. Lett. **66**, 3056 (1991).
[21] P.F. Bagwell and M. Alam, in *Workshop on Physics and Computation: PhysComp '92*, edited by D. Matzke (IEEE Computer Society Press, Los Alamitos, CA, 1993).
[22] U. Sivan and Y. Imry, Phys. Rev. B **33**, 551 (1986).
[23] Th. Martin and R. Landauer, Phys. Rev. B **45**, 1742 (1992).
[24] R. Lake and S. Datta, Phys. Rev. B **46**, 4757 (1992).
[25] A.F. Andreev, Zh. Eksp. Teor. Fiz. **46**, 1823 (1964) [Sov. Phys. JETP **19**, 1228 (1964)]; **49**, 655 (1966) [**22**, 455 (1966)].
[26] I.O. Kulik and A.N. Omel'yanchuk, Fiz. Nizk. Temp. **18**, 819 (1992) [Sov. J. Low Temp. Phys. **18**, 819 (1992)]; E.N. Bogachek and I.O. Kulik, *ibid.* **18**, 785 (1992) [**18**, 556 (1992)].